Progress In Electromagnetics Research M, Vol. 37, 149–160, 2014

Pattern Synthesis for Large Planar Antenna Arrays Using a Modified Alternating Projection Method

Dan Hua*, Wentao Li, and Xiaowei Shi

Abstract—A pattern synthesis approach based on a modified alternating projection method for large planar arrays is presented in this paper. In the alternating projection method, pattern synthesis problem is considered as finding the intersection between two sets: the specification set and the feasible set. The former contains all the patterns that want to be obtained, while the latter contains all the patterns that can be realized. An element belongs to both sets is a solution to the problem. In this paper, a modified projection operator which varies with the iteration number is introduced because the conventional alternating projection method is known to suffer from low convergence rate and/or trapping on local optimum depending on the starting point. When the planar array has a nonuniform element layout, the unequally spaced elements are interpolated into virtual uniform elements with an interpolation of the least square sense. Then the synthesis problem is converted to the problem of a uniform array. Finally, several examples are presented to validate the advantages of the proposed method. Results show that the modified method is fast and obtains better results than the conventional one.

1. INTRODUCTION

As a key component, antenna plays an important role in radio communication systems. With the growing requirements of the system, such as strong directivity, high gain and pattern scanning ability, single antenna cannot fully meet the requirements. A direct way to solve this kind of problems is to arrange the antenna elements into an array. Due to the wide azimuth and elevation scanning capability, high gain and easy three-dimensional beamforming, large planar arrays are widely used in radar, sonar and wireless communication systems. Uniformly spaced arrays with periodic element layout and simple feeding network are often used in design of antenna arrays. When compared with uniform array, nonuniform arrays can provide practical advantages such as reductions in the size, weight and number of antenna elements. Therefore the application of both uniform and nonuniform planar arrays has been an attractive topic in antenna area for some years.

In the literature, various pattern synthesis techniques can be found. The stochastic methods, such as genetic algorithm (GA) [1–4], particle swarm optimization (PSO) method [5–9], simulated annealing (SA) method [10–12] and some hybrid methods [13–16], are global optimization algorithms which can jump out from local optimum by introducing random variables. These techniques are capable of synthesizing arrays with arbitrary element layout (linear, planar and conformal arrays). While difficulties still exist, for example, the associated computation time to good result is very large and/or the array size is often small.

In recent years, a fast synthesis approach called the Iterative Fourier Technique (IFT) [17, 18] has been successfully applied to synthesize large planar arrays with less computational time. However, this Iterative Fourier technique needs all the elements placed along a uniform grid. For the synthesis of unequally spaced arrays, an analytical technique was presented by Kumar in [19], the method originally

Received 12 May 2014, Accepted 19 July 2014, Scheduled 24 July 2014

* Corresponding author: Dan Hua (hd19901002@126.com).

The authors are with the Science and Technology on Antenna and Microwave Laboratory, Xidian University, Xi'an, Shaanxi 710071, China.

employed a uniformly spaced array in any geometry, and synthesized a target pencil beam pattern by alternating the uniform spacing of the array. In [20], a well-structured mathematical formulation for nonuniformly spaced arrays was introduced by Ishimaru, who used the Poisson sum expansion of the array factor and some simplifying assumptions to derive a relationship between the pattern and element spacings to reduce the sidelobe level. In [21], Oraizi considered the nonzero phase term in Ishimaru's formula to make it capable of synthesizing any type of pattern, such as sum, different and shaped beams by nonuniform spacings and/or element phase control. Recently, approaches based on the fast nonuniform Fourier transform (NUFFT) have also been used for the synthesis of large nonuniform arrays [22–24]. While in most of these works, the main goal was only the sidelobe level reduction.

As a numerical iterative method, alternating projection method is simple, fast and easy to implement on software. And it has been successfully applied to array pattern synthesis [25–28]. Based on the concept of projection, pattern synthesis problem is formulated as finding the intersection between two sets: the specification set and the feasible set. The former contains all the patterns that want to be achieved, while the latter contains all the patterns that can be realized. An element belongs to both sets is a solution to the problem. The process of the method can be summarized as: first, choose initial values; second, compare the calculated pattern with the prescribed target one and modify the samples which exceed the limitations; third, inversely project the modified pattern to the realized pattern set, and then obtain a renewed set of element excitations. Repeat the last two steps until there is no sample to be modified or the iteration reaches its maximum number.

As the conventional alternating projection method suffers from low convergence rate and/or trapping on local optimum depending on the starting point, we introduce a modified projection operator which varies with the iteration number in the present work. The modified alternating projection method is suitable for large planar antenna arrays with arbitrary element layout (uniform or nonuniform) and capable of synthesizing patterns with any shape. When the antenna elements are irregular arranged, the nonuniformly spaced elements are interpolated into virtual uniform elements with an interpolation of the least square sense [29]. Then the synthesis problem is converted to the problem of a uniform array. Finally, the synthesis of both uniform and nonuniform array is presented to illustrate the advantages of the proposed method.

This paper is organized as follows. Section 2 presents in detail the synthesis approach for large planar arrays. It can be divided into two parts: Section 2.1 elaborates the approach for uniform arrays, and Section 2.2 expands the approach for nonuniform arrays. Section 3 shows several examples to illustrate the validity of the method. Section 4 is the conclusion.

2. DESCRIPTION OF THE METHOD

2.1. Synthesis Approach for Uniform Planar Arrays

Consider a finite two-dimensional sequence $x(m,n)$, its discrete Fourier transform (DFT) can be written as

$$X(k,l) = \sum_{m=0}^{M-1} \sum_{n=0}^{N-1} x(m,n)\, e^{-j\frac{2\pi}{M}mk} e^{-j\frac{2\pi}{N}nl} \tag{1}$$

where $k = 0, 1, \ldots, M-1$; $l = 0, 1, \ldots, N-1$.

The corresponding inverse discrete Fourier transform (IDFT) for $X(k,l)$ is

$$x(m,n) = \frac{1}{MN} \sum_{k=0}^{M-1} \sum_{l=0}^{N-1} X(k,l)\, e^{j\frac{2\pi}{M}km} e^{j\frac{2\pi}{N}ln} \tag{2}$$

where $m = 0, 1, \ldots, M-1$; $n = 0, 1, \ldots, N-1$.

For Equation (2), an equivalent expression is

$$x(s,t) = \frac{1}{MN} \sum_{k=0}^{M-1} \sum_{l=0}^{N-1} X(k,l)\, e^{j2\pi(k\cdot s + l\cdot t)} \tag{3}$$

where $s = 0, 1/M, \ldots, M-1/M$; $t = 0, 1/N, \ldots, N-1/N$.

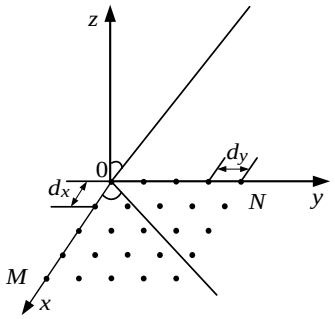

Figure 1. Element layout of uniform planar array.

Then the Fourier transformation period of s and t turns out to be 1 (M, $N \gg 1$).

An antenna array consists of M rows and N columns of elements arranged along a rectangular grid in the xoy plane is shown in Figure 1. The array has an element spacing of d_x in the x-direction and d_y in the y-direction. Ignoring the mutual coupling, the far field E can be expressed as the product of the element pattern F_e with the array factor F_a

$$E = F_e \cdot F_a \tag{4}$$

The array factor F_a can be expressed as

$$F_a(\theta, \varphi) = \sum_{m=0}^{M-1} \sum_{n=0}^{N-1} I_{mn} \cdot e^{j2\pi/\lambda(md_x \sin\theta\cos\varphi + nd_y \sin\theta\sin\varphi)} \tag{5}$$

where I_{mn} is the 2-D current distribution of the array, $2\pi/\lambda$ the wavenumber, λ the free space wavelength, and θ, φ are the elevation and azimuth angle respectively.

Clearly, the array factor (5) can be further expressed as

$$F_a(u, v) = \sum_{m=0}^{M-1} \sum_{n=0}^{N-1} I_{mn} \cdot e^{j2\pi(m\cdot k + n\cdot l)} \tag{6}$$

where $k = udx/\lambda$, $l = vdy/\lambda$, $u = \sin\theta\cos\varphi$ and $v = \sin\theta\sin\varphi$.

Obviously, (6) is similar to (3) when u, v are uniformly sampled with K, L points ($K = 2^\mu \geq M$, $L = 2^\eta \geq N$; μ, η are positive integers). Then a 2-D $K \times L$ points IDFT can be performed on I (padding by zero if necessary) to calculate the array factor (6), and then the far field E equals

$$E = F_e \cdot F_a = F_e \cdot \mathrm{IDFT}(I) \cdot MN \tag{7}$$

Generally, there is no need to multiply the Fourier result by MN, because the final pattern requires to be normalized. The visible space of the pattern expressed with k and l is

$$\left(\frac{k}{d_x}\lambda\right)^2 + \left(\frac{l}{d_y}\lambda\right)^2 \leq 1 \tag{8}$$

where $k = ud_x/\lambda$, $l = vd_y/\lambda$, $u = \sin\theta\cos\varphi$ and $v = \sin\theta\sin\varphi$. For the case, when the array has an element spacing of $d_x = d_y = \lambda/2$, the visible space turns out to be a circular region with a maximum diameter of 1.

After obtain the array pattern (7), the next is to compare the pattern with the prescribed target one and modify it following the rule:

$$|E_d(\theta, \varphi)| = P_M |E_r(\theta, \varphi)| = \begin{cases} (M_u(\theta, \varphi)/R^w), & M_u(\theta, \varphi) < |E_r(\theta, \varphi)| \\ |E_r(\theta, \varphi)|, & M_l(\theta, \varphi) \leq |E_r(\theta, \varphi)| \leq M_u(\theta, \varphi) \\ (M_l(\theta, \varphi) \times R^w), & |E_r(\theta, \varphi)| < M_l(\theta, \varphi) \end{cases} \tag{9}$$

where P_M is the positive projection operator, E_r the calculated normalized radiation pattern, E_d the modified normalized radiation pattern, $w = (1-(\mathrm{Gen}/\mathrm{Gen\_max})^n)$ a variable changes with the iteration

number, Gen the iteration number, Gen_max the maximum iteration number, and M_u and M_l are the upper and lower limitations of the required pattern. R, n are constants and satisfy $R > 0$, $n > 0$. As the iteration reaches its maximum value, that is Gen = Gen_max, the projection rule (9) turns out to be the conventional one in [26].

Then, a renewed set of element excitations can be obtained by an inverse computation of (7). Only the samples associated with the aperture (usually the former $M \times N$ samples) are retained.

$$I = \mathrm{DFT}\left(E_d / F_e\right) \tag{10}$$

The synthesis process for uniform planar arrays can be summarized as:

1) Initialize the element excitations I randomly.
2) Compute the array pattern (7) by performing a 2-D $K \times L$ points IDFT on I (padding by zero if necessary).
3) Modify the pattern obeying the rule (9).
4) Calculate and truncate the renewed element excitations I.

Repeat the steps from 2) to 4) until the pattern meets the requirements completely or the iteration reaches its maximum number. If necessary, we can also modify the obtained element excitations following the rule in [26] at the beginning of step 2).

From above, we are able to synthesize planar arrays with periodic element arrangements. For example, arrays with elements placed along a rectangular grid or arrays with elements distributed along an isosceles triangular grid can be filled into a rectangular grid with virtual elements whose excitations are set to zero. However, to reduce the cost and weight, nonuniform arrays are often adopted in array antenna designs. Due to the unequally spaced elements, the Fourier relationship derived from the array factor and the element excitations no longer holds.

2.2. Synthesis Approach for Nonuniform Planar Arrays

Supposing that a nonuniform array is placed in the xoy plane as shown in Figure 2, we mark the elements from 1 to N, then the element positions along the x-direction and the y-direction can be written as $x = [x_1, x_2, \ldots, x_N]$, $y = [y_1, y_2, \ldots, y_N]$.

The array factor F_a can be expressed as

$$F_a\left(u, v\right) = \sum_{i=1}^{N} I_n \cdot e^{j2\pi/\lambda \cdot (x_n u + y_n v)} \tag{11}$$

where $u = \sin\theta\cos\varphi$, $v = \sin\theta\sin\varphi$, $I = [I_1, I_2, \ldots, I_N]^T$ are the element excitations, and θ, φ are the elevation and azimuth angle respectively.

The array factor (11) can also be written as

$$F_a\left(s, t\right) = \sum_{n=1}^{N} I_n \cdot e^{j2\pi(P_{xn} \cdot s + P_{yn} \cdot t)} \tag{12}$$

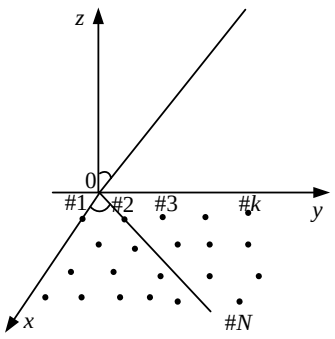

Figure 2. Element layout of nonuniform planar array.

if

$$P_{xn} = 2x_n/(N_x\lambda); \quad P_{y_n} = 2y_n/(N_y\lambda); \quad s = (N_x/2)\cdot u; \quad t = (N_y/2)\cdot v \tag{13}$$

where $P_x = [P_{x1}, P_{x2}, \ldots, P_{xN}]$ and $P_y = [P_{y1}, P_{y2}, \ldots, P_{yN}]$ are nonuniform samples and N_x, N_y are the uniformly sampling number of s and t.

Thanks for the idea of the accurate algorithm for nonuniform Fourier transforms (NUFFT's) in [29], the array factor (12) can be quickly calculated. The fast algorithm is shown in detail in [29] which is also given in brief as follows.

Consider a one-dimensional NUDFT (14)

$$H_\beta = \sum_{m=1}^{M} h_m \cdot e^{j2\pi P_m \beta} \tag{14}$$

where $P = \{P_1, P_2, \ldots, P_M\}$ are nonuniform samples. The exponential terms on the right can be approximately calculated by

$$e^{j2\pi\cdot P_m\cdot\beta} = \sum_{k=-q/2}^{q/2} a_k(c_m)\, e^{j2\pi\beta\cdot([\gamma c_m]+k)/\gamma N}\cdot d_\beta^{-1} \tag{15}$$

$$d_\beta = \cos\frac{\beta\pi}{\gamma N} \tag{16}$$

where $d_\beta > 0$ (called 'accuracy factor') are chosen to minimize the approximation error. $c_m = N\cdot P_m$, N is the number of the data points β, q an even integer, γ a real number called oversampling factor and greater than 1 (γ should be properly selected to make γN be integer), and $[x]$ the nearest integer of x.

Let $c_x = N_x\cdot P_x$ and $c_y = N_y\cdot P_y$, and then the array factor (12) equals

$$F_a(s,t) = \sum_{n=1}^{N} I_n \sum_{w_x=-q/2}^{q/2}\sum_{w_y=-q/2}^{q/2} a_{w_x}(c_{xn})\, a_{w_y}(c_{yn})\cdot e^{j2\pi(s\cdot([\gamma c_{xn}]+w_x)/(\gamma N_x)+t\cdot([\gamma c_{yn}]+w_y)/(\gamma N_y))}\cdot d_s^{-1}d_t^{-1} \tag{17}$$

where

$$\begin{gathered} d_{s,t} = \cos\frac{\pi s,t}{\gamma N_{x,y}} \quad \left(\text{or } d_s = \cos\frac{\pi s}{\gamma N_x},\ d_t = \cos\frac{\pi t}{\gamma N_y}\right) \\ a(c_{x,yn}) = \left[a_{-q/2}(c_{x,yn}), a_{-q/2+1}(c_{x,yn}), \ldots, a_{q/2}(c_{x,yn})\right]^T \end{gathered} \tag{18}$$

$a(c_{x,yn})$ are unknown complex coefficients, which can be computed by

$$a(c_{x,yn}) = F_{x,y}^{-1}\cdot g(c_{x,yn}) \tag{19}$$

where the matrix $F(\gamma, N, q)$, called the (γ, N, q) — regular Fourier matrix, is a Hermitian matrix of dimension $(q+1)\times(q+1)$. The calculation of the matrixes $F_{x,y}(\gamma, N_{x,y}, q)$ and $g(c_{x,yn})$ is given in detail in [29].

A succinct expression of (17) can be written as

$$F_a(s,t) = \sum_{k=-\gamma N_x/2}^{\gamma N_x/2-1}\sum_{l=-\gamma N_y/2}^{\gamma N_y/2-1} D_{kl}\cdot e^{j2\pi(k\cdot s/\gamma N_x + l\cdot t/\gamma N_y)}\cdot d_s^{-1}d_t^{-1} \tag{20}$$

where D denotes the element excitations of the virtual uniform array. $D = Q'\cdot I$. Q' is a two-dimensional matrix which has the same data as the three-dimensional matrix Q does.

where

$$Q_{kln} = \begin{cases} \sum a_{w_x}(c_{xn})\cdot a_{w_y}(c_{yn}), & k = ([\gamma c_{xn}]+w_x),\ l = ([\gamma c_{yn}]+w_y) \\ 0, & \text{else} \\ w_x = -q/2, -q/2+1, \ldots, q/2 & \\ w_y = -q/2, -q/2+1, \ldots, q/2 & \end{cases} \tag{21}$$

The synthesis process for nonuniform planar arrays can be summarized as:

1) Choose proper parameters γ, N_x, N_y, and q, and initialize the element excitations I randomly.
2) Calculate the complex coefficients $a(c_{x,y})$ and the matrixes Q and D.
3) Synthesize the pattern of the virtual uniform array.
4) Evaluate the element excitations of the nonuniform array: $I = Q'^{+} \cdot D$ (the subscript '+' denotes the Moore-Penrose pseudo inverse).

In the above analysis, the array pattern is calculated by the product of the element pattern and the array factor based on the presumption that all elements have equal radiation pattern; while in practical array, due to the presence of mutual coupling, the principle of pattern multiplication cannot be applied to arrays because each element "sees" different environment, and there may have significant impacts on element input impedances, array gain and shape of the pattern (such as a higher sidelobe level). Active element patterns method, which uses the measured or computed patterns of the individual elements in the array environment, can be employed to calculate the pattern of the fully excited array approximately [30].

The mutual coupling consideration for nonuniformly spaced arrays is a cumbersome work. In [31], a GA (Genetic Algorithm)-NN (Neural Network) methodology was introduced for the design optimization of broadband phased array antennas. The methodology consisted of an NN-based rapid element driving point impedance estimation technique and a rapid pattern estimation technique combined with a robust GA optimizer. It allowed for important phased array design parameters, such as sidelobe level and element VSWRs, to be determined as functions of array element positions. In [32], a novel NN-based model was presented for the computation of S-parameters. Then the GA (Genetic Algorithm)-CG (Conjugate Gradient) method can adjust these values in the synthesis process to achieve desired pattern and bearable coupling among elements. The synthesis for the specified beamwidth and minimum achievable sidelobe level were performed and the graphs which showed the relation between the beamwidth, sidelobe level and number of elements for nonuniformly spaced linear arrays were derived for the first time.

3. SYNTHESIS RESULTS

Several examples will be shown to illustrate the validity of the proposed method. For simplicity, the arrays are composed of isotropic elements, the initial element excitations are set uniformly, and the synthesis problems are unconstrained complex weighted problems.

The first example is the synthesis of a similar array as described in [17], which features a circular shaped aperture with a diameter of 33.01-wavelength. The elements are placed along a square grid as shown in Figure 1 with $d_x = d_y = 0.5\lambda$. It is a uniform array with a total element number of 3413. The synthesis target is to obtain a pattern with three flat annular sectors and four nulled sectors. The corresponding constraint region and sidelobe level (SLL) limitation is shown in Table 1.

To illustrate the impacts of the parameters R and w (in Equation (9)) on the convergence, several experiments were performed on a computer with an Intel(R) Core (TM) i3 processor operating at 3.2 GHz and equipped with 2 GB RAM. The maximum iteration number was set to 8000, and a 2-D 1024×1024 points FFTs was applied during the synthesis process.

Table 1. Sidelobe level constraints of the uniform array.

constraint region	constraint SLL
$0.076^2 \leq u^2 + v^2 \leq 0.2^2$	≤ -52 dB
$0.2^2 < u^2 + v^2 \leq 0.65^2$	≤ -78 dB
$0.65^2 < u^2 + v^2 \leq 0.999^2$	≤ -62 dB
$-03 \leq u \leq -0.15$; $0.35 \leq v \leq 0.55$	≤ -91 dB
$-0.85 \leq u \leq 0.95$; $-0.1 \leq v \leq 0.3$	≤ -87 dB
$-0.85 \leq u \leq -0.75$; $-0.4 \leq v \leq 0.1$	≤ -92 dB
$0.4 \leq u \leq 0.5$; $-0.4 \leq v \leq 0.1$	≤ -94 dB

Table 2. Synthesized results of different R (or L) and w (or n). L is an equal value of R measured in dB, $L = 20 \times lg\ R$; $w = 1 - (\text{Gen}/\text{Gen\_max})^n$, n denotes the exponent; E: the obtained radiation pattern; E_0: the required radiation pattern.

L	w or n		Total points unsatisfied	Max($\lvert E\rvert - \lvert E_0\rvert$) (dB)	Max((($\lvert E\rvert - \lvert E_0\rvert$)/$\lvert E_0\rvert$)^2)	$\Delta = \sum((\lvert E\rvert - \lvert E_0\rvert)/\lvert E_0\rvert)^2$
	w	1	32464	11.6273	7.9179	406.5548
10	w	1	417	8.2324	2.4964	5.3332
	n	0.5	5634	8.7236	2.9933	18.2487
		1	2965	8.0400	2.3210	9.4764
		2	1566	7.5336	1.9060	5.9484
20	w	1	189	7.4836	1.8684	3.5131
	n	0.5	2255	7.6998	2.0351	7.2113
		1	919	6.9135	1.4800	4.0550
		2	432	6.4680	1.2266	2.8616
30	w	1	123	6.9896	1.5278	2.6417
	n	0.5	1146	7.0427	1.5619	4.5146
		1	503	6.3971	1.1851	2.8299
		2	287	6.1002	1.0372	2.1780

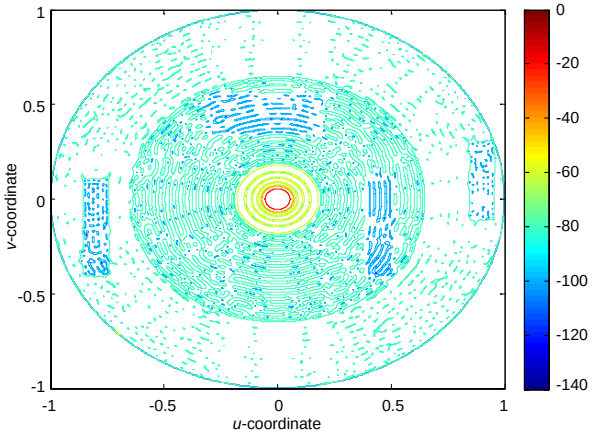

Figure 3. Contour plot of the synthesized radiation pattern.

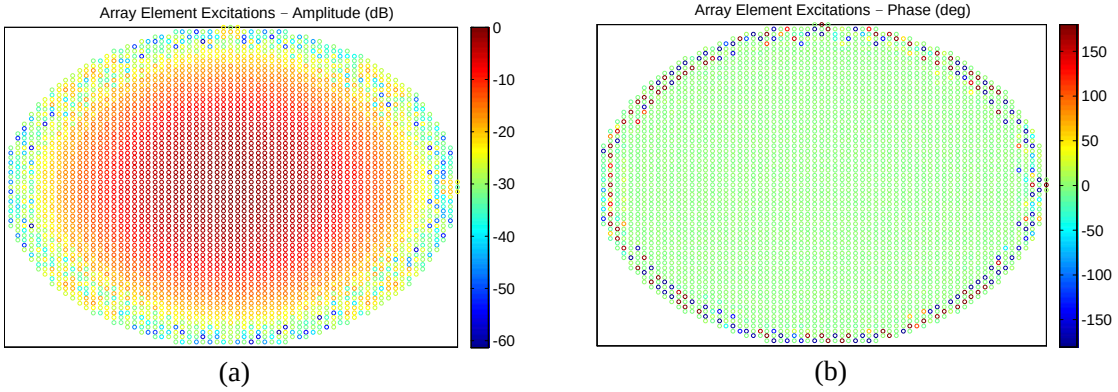

Figure 4. Aperture amplitude and phase distribution pertaining to the pattern of Figure 3. (a) Amplitude. (b) Phase.

Table 2 shows the synthesized results of different R (or L) and w (or n). The number of the samples which exceed the limitations is shown in the third column (the total number of the samples is 1050625). The fourth column gives the maximum SLL difference between the obtained and the required magnitude (measured in dB). In our tests, the maximum difference happened in the position $u = -0.8496$, $v = -0.3984$ (the required $SLL \leq -92$ dB).

The constant R (or L) was selected to make the modified samples much closer to the required. From the results shown in Table 2, it can be noted that the number of the unsatisfied samples decreases with R (or L) increases, and the impact becomes smaller and smaller when R increases, so we chose a maximum R equals to $10^{(30/20)}$ in our tests; when w is a constant, the synthesized result may easily trap into a local optimization solution, so an adaptive w which varies with the iteration number ($w = 1-(\text{Gen}/\text{Gen\_max})^n$) was adopted during our tests, and the result turned out to be better when n increases. Finally, we obtained an optimal set of parameters: $R = 10^{(30/20)}$, $w = 1-(\text{Gen}/\text{Gen\_max})^2$.

The contour plot of the synthesized radiation pattern is shown in Figure 3. This pattern has a directivity of 37.86 dB, and the 3 dB beamwidth is 2.6° in both $u = 0$ and $v = 0$ plane. The computational time was about 36 minutes with a taper efficiency of 0.5136. The amplitude distribution of the element excitations is depicted in Figure 4(a), and the corresponding phase distribution is shown in Figure 4(b).

Figures 5 and 6 depict the u-cut and v-cut of the synthesized pattern through the main beam peak. The result obtained by the conventional alternating projection method is also added to the figures. The solid line plots the result obtained by the conventional alternating projection method, and the dotted line plots the result obtained by our modified one. Obviously, the modified method speeds up the convergence and obtains better radiation pattern than the original one.

The second example is the synthesis of a concentric ring array. The element layout is shown in Figure 7. There are $[2\pi n]$ elements uniformly distributed on the nth ring with a radius of $0.5n\lambda$, and the first element on each ring is always placed along the x-direction ($n \geq 1$, $[x]$ denotes the nearest integer

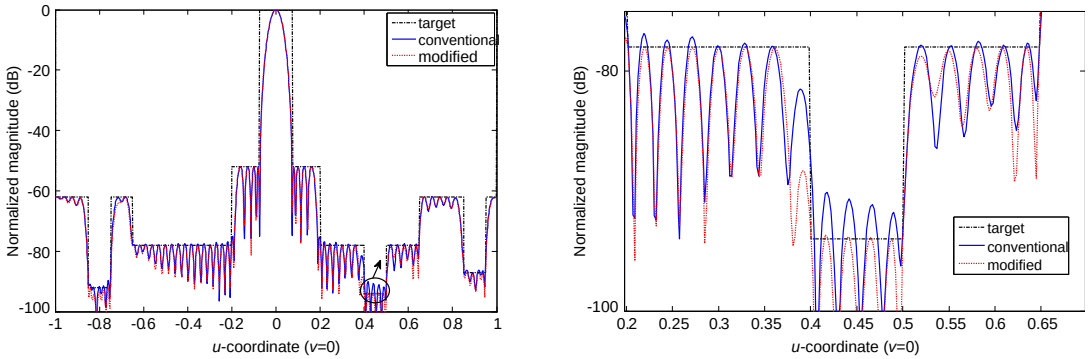

Figure 5. U-cut at $v = 0$ of the pattern of Figure 3. (a) Overall view. (b) Partial view.

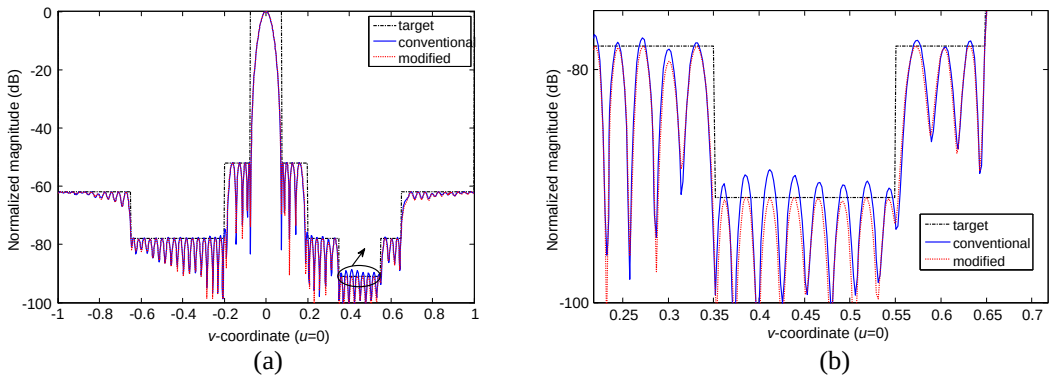

Figure 6. V-cut at $u = 0$ of the pattern of Figure 3. (a) Overall view. (b) Partial view.

less than or equal to x).

The array is composed of 25 concentric rings and an additional single element located at the center. It is a nonuniform array with an element number of 2030. The example was performed on a computer with an Intel(R) Xeon (R) X5550 processor operating at 2.67 GHz and equipped with 67 GB RAM. The parameters γ, q were chosen as 2, 12 respectively.

First, it was the synthesis of obtaining a pattern with a low sidelobe level. The maximum iteration number was set to 5000, and a 2-D 2048×2048 points FFTs was applied during the process. Finally, the pattern had a directivity of 36.61 dB, and the 3 dB beamwidth was 3° in both $u = 0$ and $v = 0$ plane.

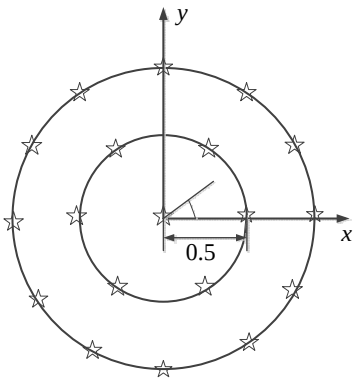

Figure 7. Element layout of the concentric ring array.

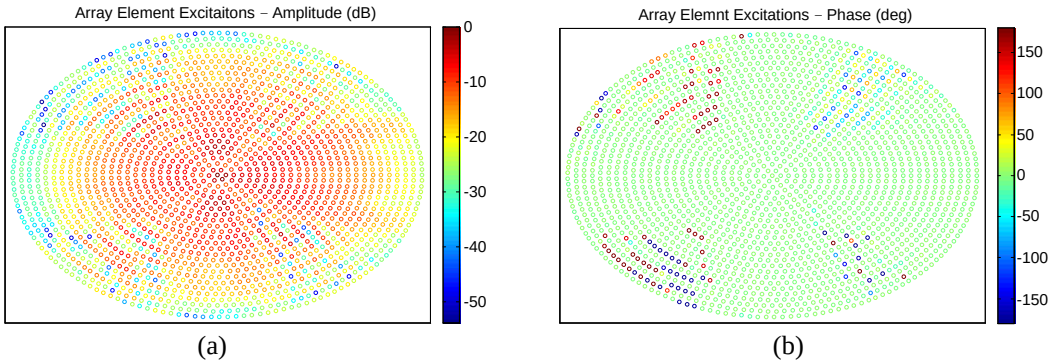

Figure 8. Aperture amplitude and phase distribution pertaining to the synthesized pattern. (a) Amplitude. (b) Phase.

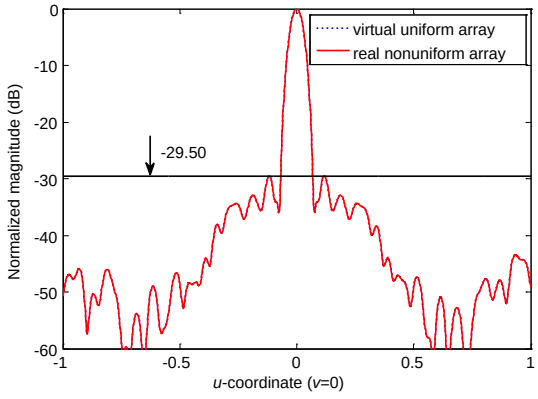

Figure 9. U-cut at $v = 0$ of the pattern.

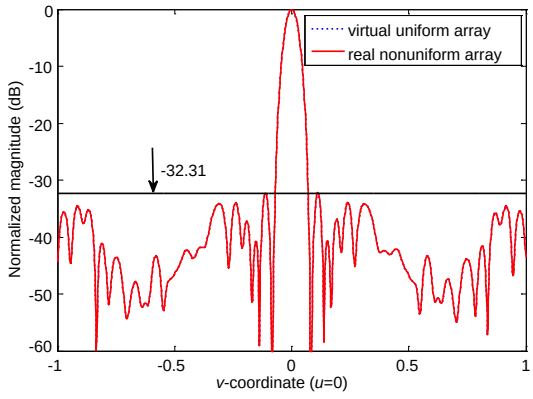

Figure 10. V-cut at $u = 0$ of the pattern.

The computational time was about 75 minutes with a taper efficiency of 0.5805. The amplitude distribution of the element excitations is depicted in Figure 8(a), and the corresponding phase distribution is shown in Figure 8(b).

Figures 9 and 10 depict the u-cut and v-cut of the synthesized radiation pattern through the beam peak direction. The maximum SLL in these two cuts is -29.5 dB and -32.31 dB respectively. To illustrate the interpolation accuracy, the pattern of the nonuniform array calculated by direct summation is also added to the figures. The solid line plots the result obtained by direct summation, and the dotted line plots the result calculated by the fast algorithm in [29].

Second, it was the synthesis of obtaining a pattern with three annular sectors. The constraint region and sidelobe level limitation is: $\{0.06^2 \le u^2+v^2 \le 0.2^2\}$, $SLL \le -32$ dB; $\{0.2^2 < u^2+v^2 \le 0.65^2\}$, $SLL \le -45$ dB; $\{0.65^2 < u^2+v^2 \le 1\}$, $SLL \le -50$ dB. The maximum iteration number was set to 20000, and a 2-D 2048×2048 points FFTs was applied during the process.

Finally, the pattern had a directivity of 37.21 dB, and the 3 dB beamwidth was 2.8° in both u-cut and v-cut. The computational time was about 3.9 hours with a taper efficiency of 0.7366. The amplitude distribution of the element excitations is depicted in Figure 11(a), and the corresponding phase distribution is shown in Figure 11(b).

Figures 12 and 13 depict the u-cut and v-cut of the synthesized radiation pattern through the main beam peak. From the two figures, it is easy to observe that there are a few samples exceed the limitations, and it's certain to get better result if we raise the iteration number and/or start with better initial element excitations.

From the results shown in Figures 9, 10, 12 and 13, it can be noted that the pattern of the virtual uniform array is almost exactly the same with that of the real nonuniform array, which indicates that the value of the parameters γ and q selected in our examples is appropriate and the interpolation is accurate.

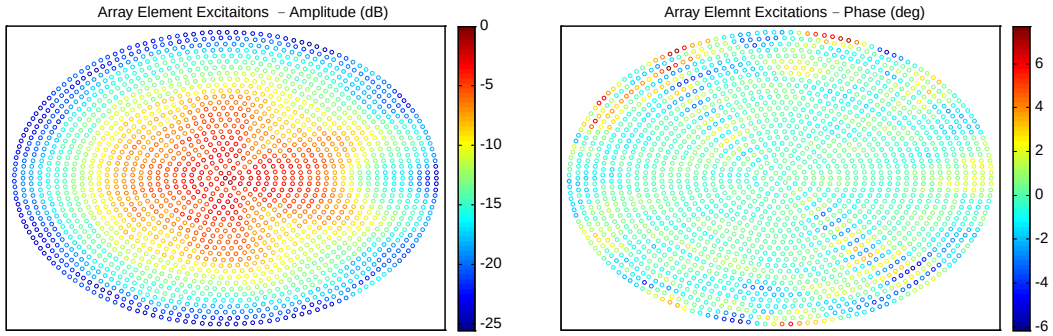

Figure 11. Aperture amplitude and phase distribution pertaining to the synthesized pattern. (a) Amplitude. (b) Phase.

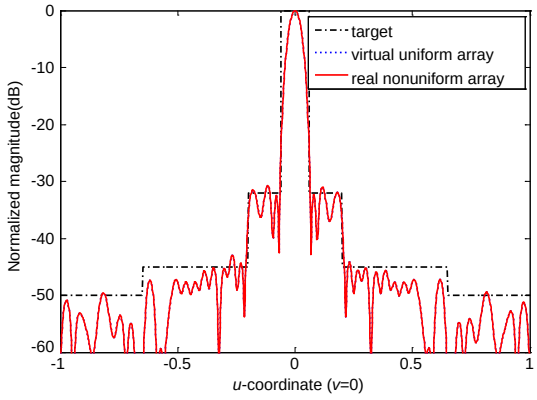

Figure 12. U-cut at $v = 0$ of the pattern.

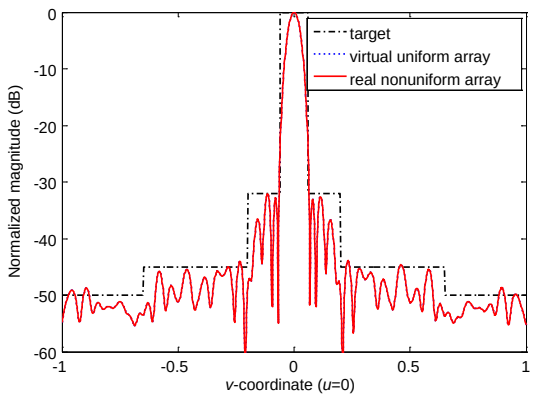

Figure 13. V-cut at $u = 0$ of the pattern.

4. CONCLUSION

A modified alternating projection method for the synthesis of large planar arrays has been presented in this paper. The method is capable of synthesizing patterns with arbitrary structure. To synthesize various pattern structures, the only thing need to do is to alter the upper and lower limitations of the target. The method can also be applied to correct array far-field patterns, which are degraded by element failures. The time complexity of the synthesis is proportional to the number of the Fourier sampling points and the iteration. To ensure accuracy, large sampling number is necessary. Therefore, it needs to trade off between the accuracy and the computation cost. In the pattern synthesis problems, the required iteration number is not related to the size of the array, but mainly depends on the level of the prescribed sidelobe level. Several examples have been presented to illustrate the accuracy and efficiency of the method. Among these examples, the element positions are pre-defined. Since the optimization of the element spacings in an aperiodic array has the benefit of increasing the degrees of freedom that are available to the designer, our future work will focus on how to obtain both appropriate element spacings and excitations to receive better radiation performance.

REFERENCES

1. Villegas, F. J., "Parallel genetic-algorithm optimization of shaped beam coverage areas using planar 2-D phased arrays," *IEEE Transactions on Antennas and Propagation*, Vol. 55, No. 6, 1745–1753, 2007.
2. Mandal, D. and Y. N. Tapaswi, "Radiation pattern synthesis of linear antenna arrays by amplitude tapering using Genetic Algorithm," *IEEE Applied Electromagnetics Conference (AEMC)*, 1–6, Kolkata, India, Dec. 2011.
3. Cen, L., Z. L. Yu, and W. Ser, et al., "Linear aperiodic array synthesis using an improved genetic algorithm," *IEEE Transactions on Antennas and Propagation*, Vol. 60, No. 2, 895–902, 2012.
4. Mandal, D. and A. K. Bhattacharjee, "Synthesis of cosec 2 pattern of circular array antenna using genetic algorithm," *International Conference on IEEE Communications, Devices and Intelligent Systems (CODIS)*, 546–548, Kolkata, India, Dec. 2012.
5. Boeringer, D. W. and D. H. Werner, "Particle swarm optimization versus genetic algorithms for phased array synthesis," *IEEE Transactions on Antennas and Propagation*, Vol. 52, No. 3, 771–779, 2004.
6. Mandal, D., S. Das, and S. Bhattacharjee, et al., "Linear antenna array synthesis using novel particle swarm optimization," *IEEE Symposium on Industrial Electronics & Applications (ISIEA)*, 311–316, Penang, Malaysia, Oct. 2010.
7. Li, W. T., Y. Q. Hei, and X. W. Shi, et al., "An extended particle swarm optimization algorithm for pattern synthesis of conformal phased arrays," *International Journal of RF and Microwave Computer-Aided Engineering*, Vol. 20, No. 2, 190–199, 2010.
8. Wang, W. B., Q. Y. Feng, and D. Liu, "Application of chaotic particle swarm optimization algorithm to pattern synthesis of antenna arrays," *Progress In Electromagnetics Research*, Vol. 115, 173–189, 2011.
9. Wang, W. B., Q. Y. Feng, and D. Liu, "Synthesis of thinned linear and planar antenna arrays using binary PSO algorithm," *Progress In Electromagnetics Research*, Vol. 127, 371–387, 2012.
10. Ferreira, J. A. and F. Ares, "Pattern synthesis of conformal arrays by the simulated annealing technique," *Electronics Letters*, Vol. 33, No. 14, 1187–1189, 1997.
11. Girard, T., R. Staraj, E. Cambiaggio, et al., "A simulated annealing algorithm for planar or conformal antenna array synthesis with optimized polarization," *Microwave and Optical Technology Letters*, Vol. 28, No. 2, 86–89, 2001.
12. Tang, W. and Y. Zhou, "Frequency invariant power pattern synthesis for arbitrary arrays via simulated annealing," *Electronics Letters*, Vol. 46, No. 25, 1647–1648, 2010.
13. Li, W. T., X. W. Shi, Y. Q. Hei, et al., "A hybrid optimization algorithm and its application for conformal array pattern synthesis," *IEEE Transactions on Antennas and Propagation*, Vol. 58, No. 10, 3401–3406, 2010.

14. Hussein, A. H., H. H. Abdullah, and A. M. Salem, et al., "Optimum design of linear antenna arrays using a hybrid MoM/GA algorithm," *IEEE Antennas and Wireless Propagation Letters*, Vol. 10, 1232–1235, 2011.
15. Bai, Y. Y., S. Q. Xiao, C. R. Liu, et al., "A hybrid IWO/PSO algorithm for pattern synthesis of conformal phased arrays," *IEEE Transactions on Antennas and Propagation*, Vol. 61, No. 4, 2328–2332, 2013.
16. Yang, J., W. T. Li, X. W. Shi, et al., "A hybrid ABC-DE algorithm and its application for time-modulated arrays pattern synthesis," *IEEE Transactions on Antennas and Propagation*, Vol. 61, No. 11, 5485–5495, 2013.
17. Keizer, W. P. M. N., "Fast low-sidelobe synthesis for large planar array antennas utilizing successive fast Fourier transforms of the array factor," *IEEE Transactions on Antennas and Propagation*, Vol. 55, No. 3, 715–722, 2007.
18. Keizer, W. P. M. N., "Low-sidelobe pattern synthesis using iterative fourier techniques coded in MATLAB," *IEEE Antennas and Propagation Magazine*, Vol. 51, No. 2, 137–150, 2009.
19. Kumar, B. P. and G. R. Branner, "Generalized analytical technique for the synthesis of unequally spaced arrays with linear, planar, cylindrical or spherical geometry," *IEEE Transactions on Antennas and Propagation*, Vol. 53, No. 2, 621–634, 2005.
20. Ishimaru, A., "Theory of unequally-spaced arrays," *IRE Transactions on Antennas and Propagation*, Vol. 10, No. 6, 691–702, 1962.
21. Oraizi, H. and M. Fallahpour, "Sum, difference and shaped beam pattern synthesis by non-uniform spacing and phase control," *IEEE Transactions on Antennas and Propagation*, Vol. 59, No. 12, 4505–4511, 2011.
22. Yang, K., Z. Q. Zhao, and Q. H. Liu, "Fast pencil beam pattern synthesis of large unequally spaced antenna arrays," *IEEE Transactions on Antennas and Propagation*, Vol. 61, No. 2, 627–634, 2013.
23. Wang, X. K., Y. C. Jiao, and Y. Y. Tan, "Synthesis of large thinned planar arrays using a modified iterative Fourier technique," *IEEE Transactions on Antennas and Propagation*, Vol. 62, No. 4, 1564–1571, 2014.
24. Liu, J., Z. Zhao, K. Yang, et al., "A hybrid optimization for pattern synthesis of large antenna arrays," *Progress In Electromagnetics Research*, Vol. 145, 81–91, 2014.
25. Poulton, G. T., "Antenna power pattern synthesis using method of successive projections," *Electronics Letters*, Vol. 22, No. 20, 1042–1043, 1986.
26. Bucci, O. M., G. D. 'Elia, G. Mazzarella, and G. Panariello, "Antenna pattern synthesis: A new general approach," *Proceedings of the IEEE*, Vol. 82, No. 3, 358–371, 1994.
27. Zhao, F., S. Chai, H. Qi, et al., "Hybrid alternate projection algorithm and its application for practical conformal array pattern synthesis," *Systems Engineering and Electronics*, Vol. 23, No. 5, 625–632, 2012.
28. Han, G. D., W. Wu, and B. Du, "Perturbation alternating projections method for pattern synthesis of phased array antenna," *IEEE Global Symposium on Millimeter Waves (GSMM)*, 385–388, Harbin, China, May 2012.
29. Liu, Q. H. and N. Nguyen, "An accurate algorithm for nonuniform fast Fourier transforms (NUFFT's)," *IEEE Microwave and Guided Wave Letters*, Vol. 8, No. 1, 18–20, 1998.
30. Kelley, D. F. and W. L. Stutzman, "Array antenna pattern modeling methods that include mutual coupling effects," *IEEE Transactions on Antennas and Propagation*, Vol. 41, No. 12, 1625–1632, 1993.
31. DeLuccia, C. S. and D. H. Werner, "Nature-based design of aperiodic linear arrays with broadband elements using a combination of rapid neural network estimation techniques and genetic algorithms," *IEEE Transactions on Antennas and Propagation Magazine*, Vol. 49, No. 5, 13–23, Oct. 2007.
32. Oraizi, H. and M. Fallahpour, "Nonuniformly spaced linear array design for the specified beamwidth/sidelobe level or specified directivity/sidelobe level with mutual coupling considerations," *Progress In Electromagnetics Research M*, Vol. 4, 185–209, 2008.